Quantifying Spatiotemporal Greenhouse Gas Emissions Using Autonomous Surface Vehicles

Matthew Dunbabin
Institute for Future Environments, Queensland University of Technology (QUT), Brisbane, Queensland 4000, Australia
Alistair Grinham
School of Civil Engineering, University of Queensland, St. Lucia, Queensland 4072, Australia
e-mail: a.grinham@uq.edu.au

Received 3 December 2015; accepted 1 June 2016

Accurately quantifying total greenhouse gas emissions (e.g., methane) from natural systems such as lakes, reservoirs, and wetlands requires the spatial and temporal measurement of both diffusive and ebullitive (bubbling) emissions. Ebullitive emissions exhibit high spatial and temporal variability and as such are difficult to measure. Traditional manual measurement techniques provide only limited localized assessment of methane flux, often introducing significant errors when extrapolated to the *whole-of-system*. This is further exacerbated when *whole-of-region* estimates are developed for inclusion in global greenhouse gas inventories. In this paper, we directly address these current sampling limitations by comparing two robot boat-based sampling systems with complementary sensing modalities to directly measure in real time the spatiotemporal release of methane to atmosphere across inland waterways. The first system consists of a single Autonomous Surface Vehicle (ASV) fitted with an Optical Methane Detector with algorithms to exploit the robot's mobility and transect repeatability for the accurate detection and quantification of methane bubbles across whole-of-system. The second system consists of multiple networked ASVs capable of persistent operation and scalable to whole-of-region monitoring. Each ASV carries a novel automated chamber-based gas sampling system to allow simultaneous real-time measurement of methane across the waterway. These ASV systems provide a foundation for persistent large-scale spatiotemporal sampling allowing scientists to develop whole-of-region greenhouse gas estimates and greatly improve global inventory budgets. An overview of the single and multi-robot sampling systems is presented, including their automated methane detection and sampling methodologies for the spatiotemporal quantification of greenhouse gas release to atmosphere. Experimental results are shown demonstrating each system's ability to autonomously navigate, detect, and quantify methane release to atmosphere across an entire inland reservoir.

1. INTRODUCTION

Quantification of greenhouse gas emissions to atmosphere is becoming an increasingly important requirement for scientists and managers to understand their total carbon footprint. Methane in particular is a powerful greenhouse gas, approximately 34 times higher global warming potential than carbon dioxide. Water storages are known emitters of methane to atmosphere (Louis, Kelly, Duchemin, Rudd, & Rosenberg, 2000). The spatiotemporal variability of releases is dependent on many environmental and biogeochemical parameters, such as hydrostatic pressure and carbon loading (Joyce & Jewell, 2003). To accurately quantify this greenhouse gas release, long duration and repeat monitoring of the entire water body is required.

Direct correspondence to Matthew Dunbabin, email: m.dunbabin@qut.edu.au

There are two primary pathways for methane to be released from water storages: (1) diffusion, and (2) ebullition (or bubbling). Diffusion is the most common pathway considered due to greater consistency (homogeneity) across a waterway. Rates of methane ebullition represent a notoriously difficult emission pathway to quantify with highly variable spatial and temporal changes (Grinham, Dunbabin, Gale, & Udy, 2011). However, the importance of bubbling fluxes in terms of total emissions is increasingly recognized from a number of different globally relevant natural systems including lakes, reservoirs, and wetlands (Bastviken et al., 2011).

Methane flux rates to atmosphere are generally expressed as a mass rate per unit area (e.g., mg m^{-2} d^{-1}). Quantifying rates due to ebullition is difficult as they are controlled by both biological and physical processes. The biological process of methanogenesis produces methane in the anoxic sediment zone (Borrel et al., 2011) and leads to supersaturation of sediment pore-waters and subsequent

(a) (b)

Figure 1. (Left) The multi-robot *Inference* Robotic Adaptive Sampling System. (Right) The *Wivenhoe* ASV on Little Nerang Dam, Queensland.

bubble formation (Boudreau et al., 2005). Physical processes can act to reduce sediment bed pressure allowing bubble release from sediment zone and then travel rapidly to the surface waters. Reduction of sediment bed stress can occur by lowering of atmospheric pressure and surface water levels, as well as internal wave dynamics (Joyce & Jewell, 2003). Conversely, increasing sediment bed pressure will act to reduce the probability of bubbling.

The dynamic influence on ebullition control processes can result in rapid (sometimes hourly) changes in both the area and intensity of bubbling (Maeck, Hofmann, & Lorke, 2014). To estimate total emissions from systems in which ebullition is the dominant contributor, the monitoring framework must account for these dynamics changes in bubbling area and intensity (Grinham et al., 2011). Modeled estimates are currently unlikely to provide a viable alternative to estimating ebullition rates as the rate of change in the control process can exceed those of modeled time-steps. Another factor that can introduce error into estimates is the variability of methane content in bubbles as they break the water surface (Crawford et al., 2014; McGinnis, Greinert, Artemov, Beaubien, & Wuest, 2006). Persistent measurement of direct methane emissions represents the optimal monitoring framework to obtain confident estimates of total emissions from these systems. This also represents a critical challenge to current manual survey efforts to quantify these spatiotemporal greenhouse gas emissions and reduce the uncertainty associated with bubbling fluxes. This is where robotics can play a significant role.

In this work, two autonomous surface vehicle-based systems designed for direct measurement of the diffusive and ebullitive methane flux and an ability to persistently and repeatedly monitor a wide spatial area are presented and compared. The first system named the *Wivenhoe* ASV consists of a 5 m long robotic catamaran to provide payload capacity for autonomously moving an optical methane detector (OMD) around the waterways for direct measurement of changes in atmospheric methane concentration due to ebullition (Figure 1(b)). This system is assumed most accurate for whole-of-system ebullition detection, as it is capable of rapid and precise surveys across large areas. However, the *Wivenhoe* ASV also represents a significant cost if persistent monitoring of a large number of systems is required (see Section 3.2.2). This will be of crucial importance when developing whole-of-region greenhouse gas emission estimates. The second system, named the *Inference* Robotic Adaptive Sampling System, consists of multiple networked robotic boats (see Figure 1(a)) and provides an open architecture allowing researchers to evaluate new sampling algorithms with customizable scientific payloads on real-world processes over extended periods of time.

The contributions presented in this paper are (1) the development of a new multi-robot greenhouse Gas Sampling System (GSS), (2) the evaluation of a multi-robot sampling strategy with no a priori information to explore the environment, and (3) an experimental comparison between the two ASV systems for detecting and quantifying methane release to atmosphere across an entire inland water storage.

The remainder of this paper is structured as follows: Section 2 provides background information. Section 3 describes the ASVs and GSS used in this study. Section 4 describes the technical approach for the spatiotemporal quantification of methane emissions using the ASVs, with Section 5 outlining the sampling methodologies. Section 6 presents experimental results using the ASV systems on an inland water storage and a discussion of the findings and observations. Finally, Section 7 draws conclusions and discusses future research.

2. RELATED WORK

Robotic platforms capable of persistent environmental monitoring offer an efficient alternative to manual or static sensor network sampling for studying large-scale phenomena. Robotic monitoring of marine and aquatic environments has received considerable attention over the past two decades

Table I. Examples of ASVs used for environmental monitoring, focusing on operations on inland waterways.

ASV (Manufacturer)	Reference	Size (m)	Hull Type	Propulsion	Endurance	Payload (kg)	Environmental Sensors
Lutra (Platypus)	N/A	0.81 × 0.47	Mono	Propeller	3 hrs	7	Physical water samples, temperature, pH, Dissolved Oxygen, sonar
Lutra Airboat (Platypus)	Valada et al. (2012) Yoo et al. (2015)	0.81 × 0.47	Mono	Fan (x1)	1.5 hrs	3.5	Physical water samples, temperature, pH, Dissolved Oxygen, sonar
Airboat (Custom build)	(Dhariwal et al. 2007)	N/A	Mono	Fan (x1)	6 hrs	N/A	Physical water sample, temperature, fluorometer
Kingfisher (Clearpath)	(Griffith et al., 2015)	1.35 × 0.98	Catamaran	Jets (x2)	N/A	10	Camera, sonar
Q-Boat 1800P (Ocean-sciences)	Tokekar, Branson, Hook, & Isler (2013)	1.8 × 0.9	Mono	Propeller	4 hrs	30	ADCP, wireless fish tracking
MARE	Girdhar et al. (2011)	1.6 × 0.6	Catamaran	Fans (x2)	2 hrs	N/A	Camera
CatOne	Duranti (2015)	1.9 × 1.2	Catamaran	Fans (x2)	8 hrs	50	ADCP, sonar
Lizhbeth	Hitz et al. (2012)	2.5 × 1.8	Catamaran	Propellers (x2)	3 hrs	N/A	Water quality sonde(winched)
ROAZ	Ferreira et al. (2009)	4.2 × 2.2	Catamaran	Propellers (x2)	N/A	350	Sonar, LiDAR
Wivenhoe	Dunbabin, Grinham, & Udy (2009)	5.0 × 2.2	Catamaran	Propellers (x2)	24 hrs	150	Water quality sonde
Wave Glider (Liquid Robotics)	(Manley et al., 2010)	2.08 × 0.6	Mono	Wave	> 1 year	18	Meteorology, ADCP water quality sonde
C-Enduro (ASV)	Savvaris, Oh, & Tsourdos (2014)	4.1 × 2.45	Catamaran	Propeller (x2)	3 months	100	Configurable, fixed and towed

Notes: N/A = Not Available.

(Dunbabin & Marques, 2012). While most studies have focused on underwater vehicles with restricted payloads and endurance, there is now increasing focus on ASVs with greater endurance and payload carrying capacity for large-scale unsupervised environmental monitoring (Manley & Willcox, 2010; Rynne & von Ellenrider, 2008; Wang, Gu, & Zhu, 2008). These systems are primarily designed for oceanographic surveys and are not particularly suitable for relatively unexplored inland waterways with challenging and often varying navigational requirements.

Recently, a series of ASVs have been designed and used on inland waterways. Table I lists a number of these platforms, their size, and payload capacity, including a reference to their use in environmental monitoring. As seen, the styles of vehicle range from smaller monohull research class boats with endurance of a few hours (some of which are commercially available), up to larger vessels with greater payload capacity and significant endurance, typically having a catamaran hull style. For inland waterway monitoring, a number of ASV platforms have adopted a pusher fan propulsion system to try to reduce the influence of the propeller-induced turbulence on the water measurements. For this study, we have developed catamaran-style ASVs to provide the necessary payload capacity as well as to minimize obstruction of the airflow around the sensors. In addition, catamarans generally have low draft and low drag to minimize wake, which can cause surface waves, resulting in localized release of methane to the atmosphere.

Navigation around narrow inland waterways is often more challenging than navigating the ocean because of issues such as above, below, and on-water obstacles and global positioning system (GPS) reliability (e.g., in mountainous and in forested systems). All vehicles in Table I use some form of GPS and compass for waypoint navigation, with larger vehicles also adopting sensors for above and below water obstacle detection. A number of

sensors have been used to detect obstacles and to identify free-space paths. Hitz et al. (2012) use water depth only for detecting shallow regions, whereas Ferreira et al. (2009) and Leedekerken, Fallon, & Leonard (2014) use scanning laser range finders and sonar to produce high-resolution three-dimensional maps of the above- and below-water environment. Cameras have also been proposed for detecting specific objects on the water (Ferreira et al., 2009; Dunbabin et al., 2009). Scherer et al. (2012) have used cameras and laser scanners (albeit on an aerial robot) to map the edges of waterways and the free-space above the water as the robot traverses them. Although high-resolution sensors such as lasers, radar, and sonar can provide robust navigation capabilities, for persistent monitoring their power consumption can be a particular challenge. Exploiting lower power and cost, sensing modalities such as vision and ultrasonics to provide sufficient obstacle detection capabilities is a goal of our multi-robot research.

In practice, most applications of ASVs are for short-term experiments to validate existing or to generate new models (Dunbabin & Marques, 2012). Recently, cross-disciplinary research has been extensively using robots to investigate assumptions around spatiotemporal homogeneity of environmental processes, such as toxic algal blooms in lakes (Garneau et al., 2013). These studies show that combined robotic persistence and spatiotemporal sampling can provide significant new insight into environmental processes. However, there are challenges to achieving persistent robotic process monitoring, particularly in the complex environments considered here. These primarily relate to robotic platforms for persistent navigation within complex and often dynamic environments and the ability to adaptively coordinate multiple robots to appropriately sample the process of interest.

The overall coordination of the mobile sensors (robots) is critical to accurately measure spatiotemporal environmental processes. An emerging research area for ASVs is that of mobile adaptive sampling in which the ASV can alter its trajectory to improve measurement resolution in space and time (e.g., (Zhang & Sukhatme, 2007)). The survey paper of Dunbabin and Marques (Dunbabin & Marques, 2012) summarizes advances in robotic adaptive sampling for environmental monitoring. Past research has focused primarily on the Gaussian process-based reconstruction of stationary processes using combinations of mobile and static sensors networks (Zhang & Sukhatme, 2007; Hombal, Sanderson, & Blidberg, 2010). While demonstrating the ability to capture and reconstruct various parameter distributions, these studies offer simulation only or short duration small-scale experimental validation. More recent work has used multiple ASVs to experimentally compare different search strategies (e.g., random, lawn-mower) to reconstruct surface water parameters (Valada et al., 2012). Developing and demonstrating multi-robot adaptive sampling algorithms for the large-scale monitoring and tracking of spatiotemporal environmental processes, such as greenhouse gas release to atmosphere as presented here, is an overarching goal of our research.

3. ROBOTIC SAMPLING SYSTEMS

Two alternate ASV systems for the spatiotemporal detection and quantification of greenhouse gas release to atmosphere across inland waterways are discussed. The first is the Commonwealth Scientific & Industrial Research Organisation (CSIRO) developed *Wivenhoe* ASV (Dunbabin et al., 2009) whose sensor payload and processing algorithms were developed to exploit the mobility and repeatability offered by the ASV to rapidly detect and quantify methane ebullition. The second is the Queensland University of Technology (QUT) developed *Inference* Robotic Adaptive Sampling System, which has been developed to exploit robot persistence and multi-robot operations to sample, quantify and map both diffusive and ebullitive methane release to atmosphere (Dunbabin, 2015). An overview of the ASVs and associated payload systems are provided below.

3.1. The *Wivenhoe* Autonomous Surface Vehicle

3.1.1. System Overview

The *Wivenhoe* ASV is a custom developed platform capable of carrying a range of environmental sensors for measuring important environmental water quality and atmospheric parameters. The 5 m long electric-powered vehicle is capable of carrying payloads of up to 150 kg with an endurance of 24 hr (without methane sensor). The ASV's onboard navigation sensors include a scanning laser range-finder (Hokuyo, Osaka, Japan) for obstacle detection, GPS (u-blox, Thalwil, Switzerland) for position and speed, magnetic compass (LORD, Williston, USA) for heading, and water depth (Navman, New Hampshire, USA). The ASV is capable of navigating unaided throughout the complex water storage along prespecified paths and speeds and has onboard obstacle avoidance processing capabilities using a 1.4 GHz Pentium M CPU running Linux and a software architecture built on the Distributed Data eXchange framework (DDX) (Corke, Sikka, Roberts, & Duff, 2004).

Communications on the ASV is via a 2.4 GHz wireless embedded system (XBee IEEE 802.15.4) allowing serial communication between the vehicle and existing static floating sensor nodes as well as remote operators.

3.1.2. Optical Methane Detector

In this study, the *Wivenhoe* ASV was fitted with an Optical Methane Detector (OMD) sensor (Heath Consultants, Texas, USA). The OMD is a survey instrument typically used for methane leak detection in landfill sites and is capable of detecting atmospheric methane concentration as low as 1 ppm. The OMD employs an open-path infrared beam detector specific to methane and outputs a measurement every

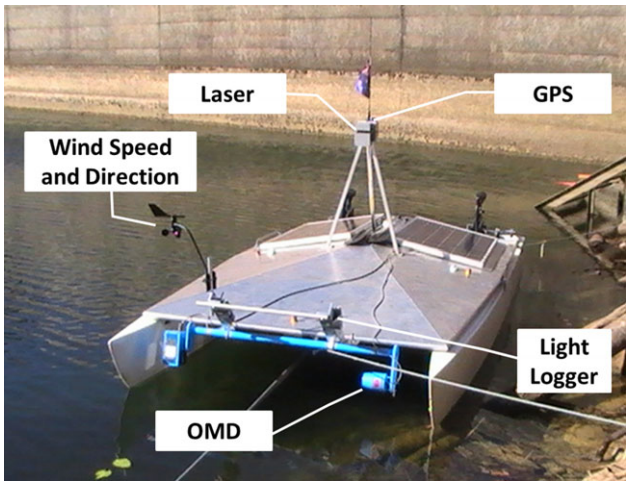

Figure 2. The *Wivenhoe* ASV illustrating the Optical Methane Detector (OMD) and the wind speed and direction sensors used for methane detection and quantification. The solar panels provide power for both propulsion and payload systems, with computing and communication hardware housed underneath the solar panels.

0.13 s (7.6 Hz). The manufacturer indicates minor cross sensitivities to propane and ethane; however, gas analysis from bubble traps at the study site revealed below detectable limits of these gases in the bubbles. This sensor weighs approximately 14 kg (without battery) and has a power requirement of 60 W.

The OMD is mounted on the front of the ASV with a sensor height of approximately 200 mm above the water surface as seen in Figure 2. To complement the OMD, two additional sensors were integrated to the ASV: (1) wind speed and direction (Davis Instruments, California, USA) and (2) a light logger (Odyssey, Christchurch, New Zealand).

This ASV and OMD sensor combination has the advantage that it can continuously measure methane while moving (see Section 4.1 for details on the real-time processing methodology), providing increased spatial coverage and repeatable measurement trajectories without human intervention. Other advantages include the low-interference of its own structure to the flow of air through the sensor compared to monohull boats. The ASV has electric propulsion, and the vehicle's draft is minimal to limit surface wave disturbances or turbulence, which could influence bubble release, particularly in the shallower regions of the water reservoir. Finally, it allows accurate georeferencing and time-stamping of all measurements for real-time and/or post-analysis. However, a limitation is that the OMD can only detect ebullition (bubbling), as diffusion only increases the local atmospheric methane concentration by <0.01 ppm, which is one order of magnitude below the resolution of the OMD.

Figure 3. One of the ASVs from the *Inference* system. The navigation sensors, computing, and batteries are located underneath the two solar panels. The scientific payload, in this study the GGS described in Section 3.2.2, is attached to the moon-pool opening underneath the camera.

3.2. The *Inference* Autonomous Surface Vehicles

3.2.1. System Overview

The multi-robot *Inference* system consists of custom-designed ASVs for persistent and cooperative operation in challenging inland waterways. The overall hull shape (see Figure 3) has four key features: (1) a low draft allowing traversal in shallow water, (2) open sides and low curved top deck to minimize windage and the associated drift when station keeping during sampling, (3) a large top surface area angled for maximizing energy harvesting from the solar panels, and (4) a moon-pool (open center section) with standardized attachment points to mount custom sensor packages. The overall dimensional and mass specifications for the ASVs, including details of the battery and propulsion systems, are presented in (Dunbabin, 2015).

These relatively low-cost ASVs are capable of carrying additional custom payloads weighing up to 10 kg. The payload is mounted under the moon-pool opening. Each ASV has a suite of low-cost navigation sensors, which include a GPS, a magnetic compass with roll and pitch, and a depth sensor for measuring bathymetry. A USB camera (Microsoft LifeCam) mounted above the moon-pool and four Maxbotix ultrasonic range sensors mounted just under the leading and trailing edges of the top deck are used for obstacle detection. These sensors are used to detect the edge of the water and at-surface structures such as reeds, trees, and water lilies. To minimize power consumption and cost, typical scanning laser-based or radar sensors are not currently used, although they can be added if required in future scenarios. To facilitate vision-based obstacle avoidance, each ASV has an Odroid C1 ARM Cortex-A5 1.5 GHz quad core CPU running the Robotic Operating System (ROS) and OpenCV.

There are two communication systems onboard the ASVs. The first is a 2.4 GHz wireless embedded system (XBee IEEE 802.15.4), allowing serial communication

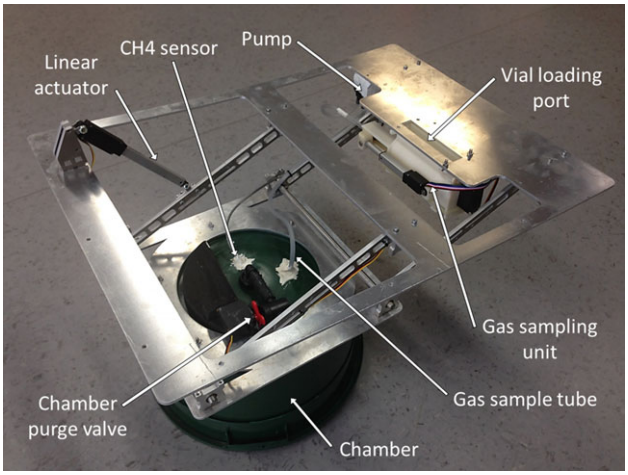

Figure 4. The GSS used to measure greenhouse gas (methane) release to the atmosphere from the inland water storages. The GSS has a total weight of 4.6 kg and is attached to moon-pool section of the ASV.

between each vehicle as well as with existing static floating sensor nodes. The second is a 2.4 GHz WiFi system allowing communication to a gateway located on a floating platform on the water storage (not used in this study).

3.2.2. Gas Sampling System

Figure 4 shows the self-contained greenhouse GSS developed to autonomously measure both the methane efflux from waterways. This payload is mounted underneath the *Inference* ASV via attachment points located around the moon-pool opening. The GSS automates the traditional manual chamber-based sampling process (Grinham et al., 2011) and consists of three primary components: (1) A frame allowing the lowering and raising of a chamber into the water, (2) a chamber fitted with a continuous methane gas (CH_4) sensor (Dynament, Mansfield, United Kingdom) and purge valve, and (3) a physical gas sampling unit. The continuous methane sensor is a miniature, lightweight (0.015 kg) and low-power (0.4 W) optical sensor using nondispersive infrared (NDIR) with a sampling resolution of 0.01 %v/v (or 100 ppm). The sampling protocol using the GSS is described in Section 4.2.

The advantages of the *Inference* ASV and GSS combination are their relatively lower cost compared to the OMD-based system and, depending on the operating/sampling scenario, their ability to persistently monitor the environment (days to months). Currently, the cost of each *Inference* ASV is approximately 6.9% of the total cost of the *Wivenhoe* ASV. Table II provides a summary of the cost of the key hardware components relative to the total cost of each ASV. As can be seen, the OMD represents the most significant cost of the *Wivenhoe* system, whereas the hull structure is most significant for the *Inference* ASV, albeit at a fraction of the total cost of the *Wivenhoe* ASV. The disadvantage when compared to the *Wivenhoe* ASV and OMD combination described above is that measurements need to be taken while the ASV is stationary, limiting the number of samples per day and the associated spatial coverage.

Table II. Comparison of the cost of key ASV hardware components relative to the total cost of both the *Wivenhoe* and *Inference* ASVs.

Item	*Wivenhoe* ASV (%)	*Inference* ASV (%)
Structure (hull)	8.7	50.2
Propulsion	1.3	6.9
Batteries	0.6	3.0
Solar panels and charger	1.0	3.0
Navigation sensors	15.2	13.9
Computing hardware	1.0	3.1
Communications	0.3	3.9
Miscellaneous hardware	0.9	6.9
Methane sensor systems	71.0	9.1
Total	100.0	100.0

3.2.3. Operating Scenario

The *Inference* Robotic Adaptive Sampling System was developed with the goal of providing a shared resource of multiple networked ASVs to allow researchers to remotely evaluate new sampling algorithms on real-world processes over extended periods of time. A typical use scenario proposed for the system is outlined below:

1. The ASVs, each carrying a scientific payload, are deployed on a water body.
2. Based on a desired sampling protocol (e.g., random, adaptive) and process modeling requirements, new sampling locations are determined. This can be achieved from either a remote centralized or an onboard decentralized process.
3. Determine which ASV goes to each of the updated sample locations. This may involve optimizing a cost function (e.g., minimizing energy and/or travel time, maximizing solar energy harvesting).
4. Each ASV navigates to its commanded sampling location.
5. Each ASV takes its scientific measurement and reports it back through the network.
6. Repeat Steps 2-5 until a termination condition is met.

The system described in this paper is working towards this goal with a preliminary experimental evaluation of this

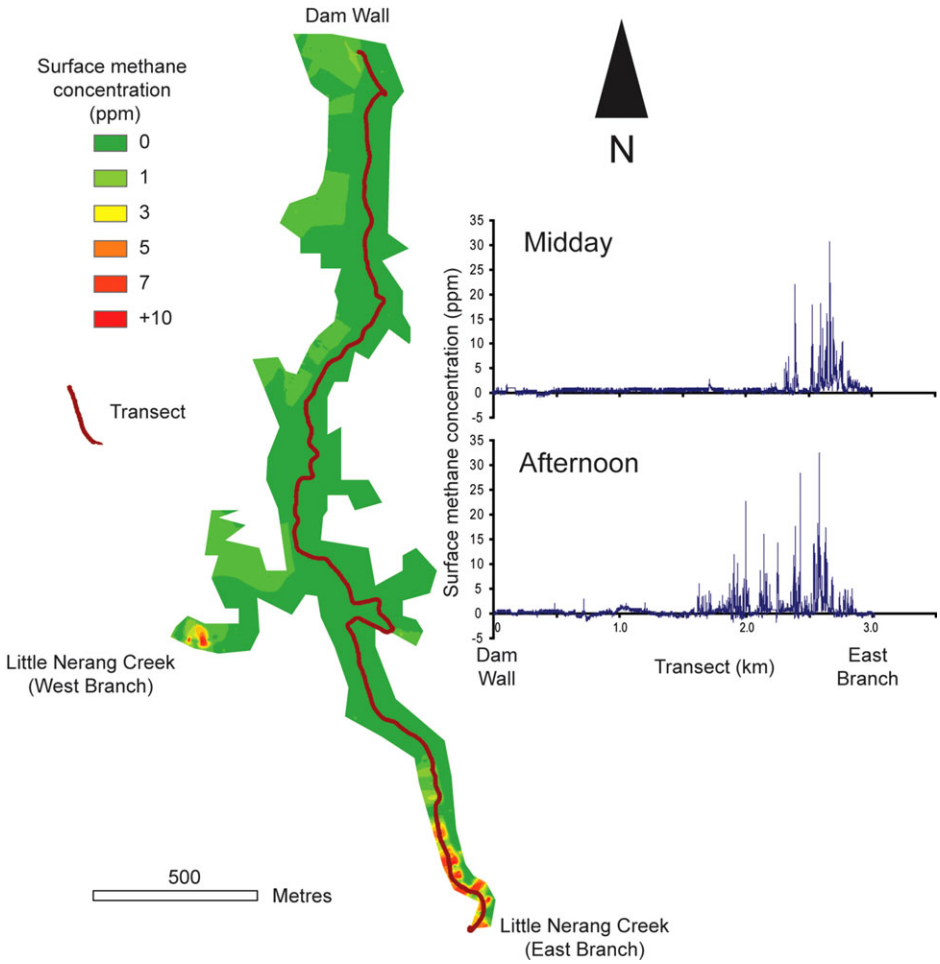

Figure 5. Example of the measured atmospheric methane concentration and variation along the same transect at different times of day using the OMD attached to a boat on Little Nerang Dam, Queensland, Australia. The spikes (increase) in the surface methane concentration result from the OMD passing through a methane bubble, which has emerged from the water's surface to atmosphere. These methane bubbles are predominantly released from the shallower Western and Eastern branches of the reservoir.

scenario using a simplified random exploration algorithm as described in Section 5.2.

4. SPATIOTEMPORAL QUANTIFICATION OF METHANE: TECHNICAL APPROACH

The goal of this study is to measure greenhouse gas emissions (efflux) across entire waterways. As the sensors considered here measure the change in atmospheric methane concentration (e.g., in parts per million), methods are required to convert the measured concentrations to a standardized flux rate in mg m^{-2} d^{-1}. Two different strategies for the quantification of methane release to atmosphere via ebullition have been developed and evaluated to complement the respective payload and navigation capabilities of the two ASV systems described in Section 3 and are discussed in the following sections.

4.1. OMD-Based Methane Bubble Detection and Volume Estimation from a Mobile Platform

The OMD provides a continuous measurement ($\approx$ 7 Hz) of methane concentration in the air passing through its optical sensor path. Whilst the sensor was originally designed for detecting methane leaks at landfill sites, we repurposed the OMD and attached it to a boat to evaluate whether it could (1) detect the presence of methane bubbles as it moved just above the water's surface and (2) if so, could the signal be used to estimate the volume and hence the rate of methane release to atmosphere via ebullition.

An initial experiment was conducted in which the sensor was attached to a boat approximately 200 mm above the waterline and driven along a track into a region where methane bubbling was visibly observed. Figure 5 shows the measured atmospheric methane concentration as the boat

moved along the track for two repeated transects (midday and afternoon) from the deeper region of the water storage to the shallower distal arm where bubbling was observable. As can be seen, when the OMD passes over a bubble event, the atmospheric methane concentration subsequently increases (spikes) before returning to background levels. In addition, it can be observed that the extent (length along the transect) of the bubbling zone varies between transects. As such, quantifying methane release to atmosphere and identifying the spatial and temporal variability of this zone using the OMD were a key focus of our work.

A methodology for correlating the measured time history from the OMD to characterize the individual bubble release from the water's surface and quantify bubble size was developed. Here, we exploit the mobility of a robotic platform to improve the spatial coverage and consistency of measurements. A Gaussian gas plume dispersion model (Beychok, 2005) is used to correlate the detected time signature of methane concentration from the OMD (Figure 5) to a series of discrete bubbles that broke at the water's surface. For detailed methodology and laboratory evaluation associated with bubble detection and volume estimation, see (Grinham et al., 2011). However, we briefly describe the critical components of these processes below.

4.1.1. Bubble Event Quantification

The methodology behind transforming the recorded time history of methane concentration through the moving OMD, which is attached rigidly to the ASV for estimating the bubble size that broke at the water's surface, is presented below. To interpret this data, a number of assumptions have been made: (a) the ASV is assumed moving in a forward direction at a known speed (note that the data during turns and while stationary is not considered in this study), (b) the principle component of flow through the sensor is parallel to the direction of travel, (c) the influence of the ASV structure on the forward flow is negligible, (d) the wind is horizontal to the water's surface at the sensor detection height and its instantaneous speed and direction is known, (e) the plume is Gaussian in the vertical distribution based on the previous section, (f) a bubble is defined as a continuous time segment that exceeds a preset methane concentration level, and (g) a bubble event is a sequence of spikes in close succession to each other but in the same continuous time segment.

The output from the OMD represents an integrated methane concentration across the optical path of the sensor. In addition, as the OMD is only sensitive to methane, we can ignore the contribution of other gases in the bubble and determine the equivalent volume of a 100% methane bubble (V) originating at the water's surface. Assuming a rectangular segment of constant methane concentration passing through the OMD, V can be estimated between the time segment ($t_s \leq t \leq t_f$) by:

$$V = \frac{1}{\rho_{CH4} \times 10^6} \int_{ts}^{tf} c_a w_z l_{omd} v dt, \tag{1}$$

where ρ_{CH4} is the density of methane at ambient conditions, c_a is the instantaneous average methane concentration in parts per million (ppm) as measured by the OMD, w_z is the vertical extent of the collapsed volume, l_{omd} is the sensor optical width, and v is the instantaneous relative velocity of gas passing through the sensor field.

To obtain a bubble volume estimate, we must map the actual distributed methane concentration of the plume to a volume of constant methane concentration. Therefore, it is assumed that the actual plume has an instantaneous Gaussian distribution in the vertical (z) direction approximated by:

$$c_z = c_k e^{\frac{-(z)^2}{2\sigma_z^2}}, \tag{2}$$

where c_k is the measured methane concentration at time k, z is the vertical distance relative to the sensing path, and σ_z is the vertical plume dispersion standard deviation determined to be $\sigma_z = 0.04$ m based on the bubble dispersion model developed in (Grinham et al., 2011).

The integral of this vertical Gaussian distribution is:

$$I_z = \int_{-\infty}^{\infty} c_z dz = c_k \sigma_z \sqrt{2\pi}. \tag{3}$$

Therefore, the vertical height of the plume assuming a rectangular distribution with constant methane concentration is:

$$w_z = \frac{I_z}{c_k} = \sigma_z \sqrt{2\pi} \tag{4}$$

Strictly, the integral should be between the water surface and plus infinity. However, as σ_z is small and there are more than 4 standard deviations from the sensor to the water's surface, then over 99.9% of the distribution is enclosed with the above approximation and is considered acceptable for this analysis.

An individual bubble (i) is defined by the continuous time segment bounded by a prespecified threshold (e.g., $c_k > 1.7$ ppm). As the measurement is discrete samples, we assume the velocity of air passing through the OMD v (compensated for vehicle and wind speed) is constant between time k and $k-1$ (approximately 0.13 s). The detected mass of methane (dm_k) passing through the OMD between time k and $k-1$ is estimated as:

$$dm_k = \rho_{CH4} \left(\frac{c_k + c_{k-1}}{2 \times 10^6} \right) w_z l_{omd} v dt, \tag{5}$$

where c_k and c_{k-1} are the current and previously measured methane concentrations in parts per million, respectively. Therefore, the total bubble mass for bubble i (m_i) is the

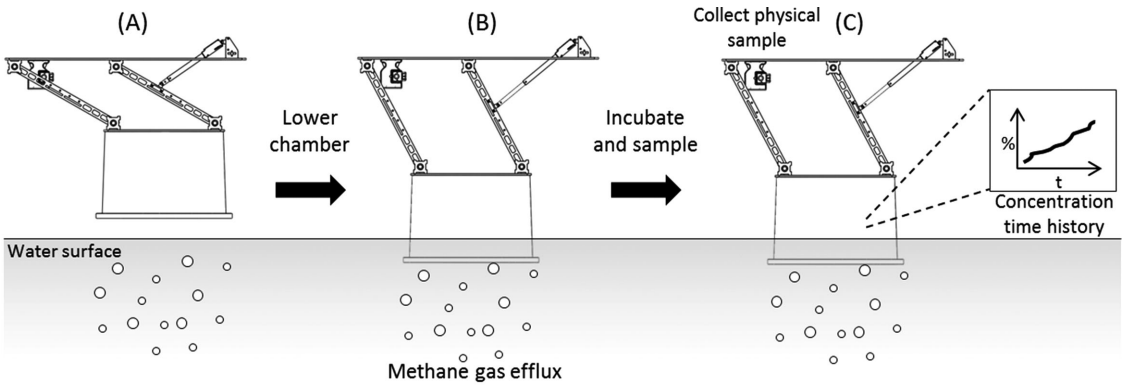

Figure 6. The sequence of actions required to measure greenhouse gas using the GSS.

sum of all detected methane values above the preset threshold bounded by ($t_{s_i} \leq t \leq t_{f_i}$), with the volume of bubble i assuming 100% methane concentration is given as:

$$V_i = \frac{m_i}{\rho_{CH_4}} \tag{6}$$

The instantaneous flux rate can be approximated by dividing the total methane bubble mass (m_i) by the time between successive bubble detections (Δt) and by the swept area of the sensor over that time ($l_{omd} v \Delta t$).

4.2. Gas Sampling System Methane Flux Quantification

The second approach for methane detection and efflux quantification considered in this study exploits the multi-robot capabilities and the persistence of the *Inference* ASVs to achieve spatial coverage. Complementing the approach of Section 4.1, the *Inference* ASVs conduct stationary measurements of gas efflux using the GSS shown in Figure 4. This method has the advantage that it measures the total methane release (ebullition and diffusion), albeit at reduced spatial coverage.

The process of sampling the greenhouse gas being released from the water to the atmosphere using the GSS is illustrated in Figure 6 and consists of four steps. First, the ASV navigates to the desired sampling location it goes into a *weak* station-keeping mode. This limits the control input to the motors to reduce any disturbance that may influence the CH_4 efflux at the expense of a slightly increased station bound. At this point, the chamber purge valve (see Figure 4) is opened and the chamber lowered using the linear actuator to achieve a desired air volume within the chamber (Figure 6(A-B)). The second step involves closing the chamber purge valve and letting the methane concentration within the chamber increase for a predetermined *incubation* time (see Section 4.2.1 for a discussion on incubation time). During incubation, the methane sensor continuously measures the concentration within the chamber (Figure 6(B-C)). At the end of the incubation, the third step (Figure 6(C)) calculates the overall gas efflux rate from the gradient of the recorded methane concentration time history. Also a physical sample of gas from the chamber can be collected for laboratory analysis using the gas sampling unit (see Figure 4). This involves a sequence of actions that first purges the sample tube using the pump and then loads a pre-evacuated 12-mL vial into the sampling unit. A linear actuator on the unit drives a hypodermic needle into the vial while pumping gas from the chamber. Once 20 mL of gas has been pumped into the vial (over pressure sampling technique), the needle retracts, and the unit discharges the vial ready for the next sample.

After sampling is completed, the final step involves opening the chamber purge valve and raising the chamber out of the water. At this point, the ASV can move to the next sample location.

4.2.1. Gas Sampling System Sampling Protocol

A key consideration for greenhouse gas sampling using the GSS is determining the minimum incubation time that maximizes detection accuracy. During the sampling phase, the concentration measured by the methane sensor is polled every 2 s for the entire incubation period. A linear least squares line of best fit is applied to this time history and the gradient used to calculate the flux rate. However, the output from the continuous methane sensor in the GSS is quantized to 0.01% (100 ppm), which is a relatively coarse measurement when compared to the OMD for estimating flux rates. While diffusive fluxes are typically less than 50 mg m^{-2} d^{-1}, ebullitive fluxes in our region can be has high as 22,000 mg m^{-2} d^{-1} (Grinham et al., 2011). Varying the incubation time and/or head-space ratio (i.e., the ratio of chamber surface area (A_c) to its internal air volume (V_c)) can be used to achieve a desired detection accuracy. Figure 7 shows the predicted variability in relative measurement error (i.e., the percentage error between a true

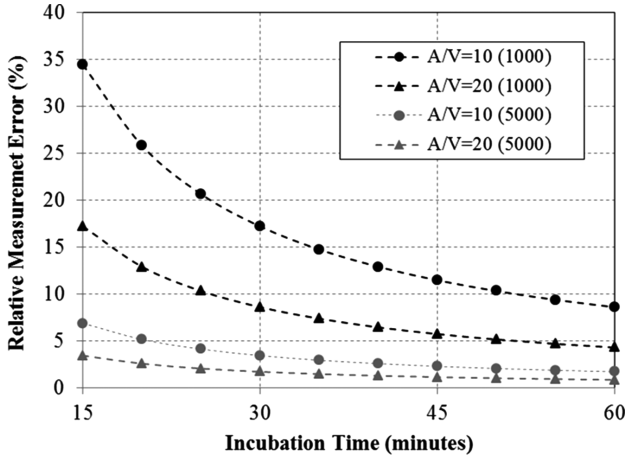

Figure 7. The predicted percentage relative measurement error of methane flux rate with incubation time for the prototype GSS (see Section 3.2.2) with a sensor output resolution of 0.01% (100 ppm). Two efflux rates are considered, 1,000 and 5,000 mg m^{-2} d^{-1} with head-space ratios (A_c/V_c) of 10 and 20 m^{-1}).

methane flux to that which can be measured by the GSS) versus incubation time for different methane efflux rates and head-space ratios. As can be seen, longer incubation times and higher efflux rates lead to reduced errors as with increasing head-space ratios. However, longer incubation times mean less sample points can be performed per day. In this study, the primary interest is the detection of methane "hot spots," that is, where it is bubbling from the water. Therefore, incubation times of 15-20 min were chosen here to allow detection of methane rates as low as 1,000 mg m^{-2} d^{-1}, albeit at lower accuracy. While increasing the head-space ratio even more will improve the detection performance, there is risk of the sensor getting too close to the water and splashed by waves. Further improvements are expected as new sensors with higher resolution also become available.

Figure 8 shows examples of raw measured time histories of methane concentration from controlled laboratory experiments using the GSS. Here, the 300 mm diameter chamber was submerged in water to give a fixed head-space ratio of 10 m^{-1} and methane gas bubbles introduced via a syringe underwater to achieve a flux rate of 1,000 and 5,000 mg m^{-2} d^{-1} for 15 min. The effect of sensor output quantization can be seen with only a 0.02% rise for the 1,000 mg m^{-2} d^{-1} over the 15 min incubation. Fitting a least squares line of best fit to the trace gives an estimated flux rate in these experiments of 1,187 and 5,192 for the inputs of 1,000 and 5,000 mg m^{-2} d^{-1}, respectively, which is consistent with Figure 7.

5. STORAGE-SCALE GREENHOUSE GAS SAMPLING METHODOLOGIES

The two ASV systems described in Section 3 exploit different sampling modalities to maximize greenhouse gas detection and quantification. The OMD-based system requires a larger vehicle to undertake repeat transects due to payload size and weight; however, it provides a continuously moving measurement. The GSS-based approach while requiring more time to collect each sample can be

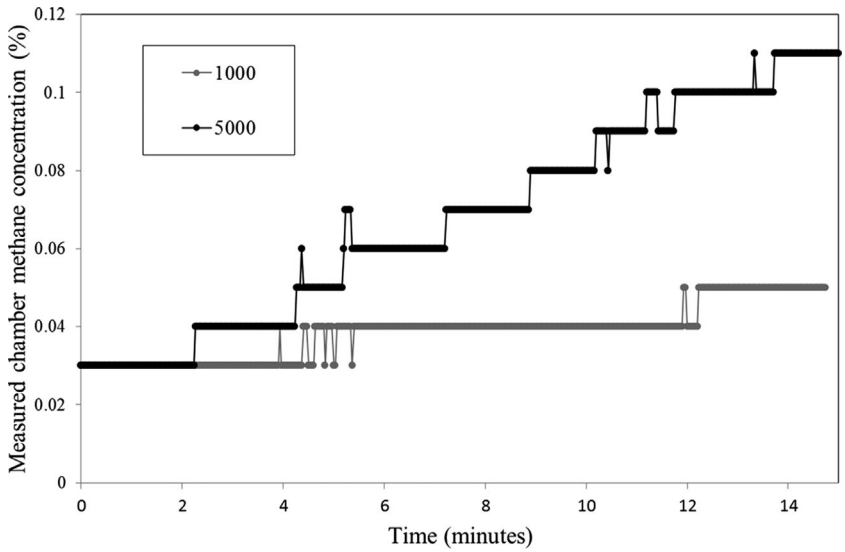

Figure 8. The raw measured methane concentration inside the GSS chamber during controlled laboratory experiments over a 15-min incubation time and head-space ratio of 10 m^{-1}. Two experiments are shown with methane gas introduced to the chamber at rate of 1,000 and 5,000 mg m^{-2} d^{-1}, respectively. The effect of sensor quantization is clearly visible.

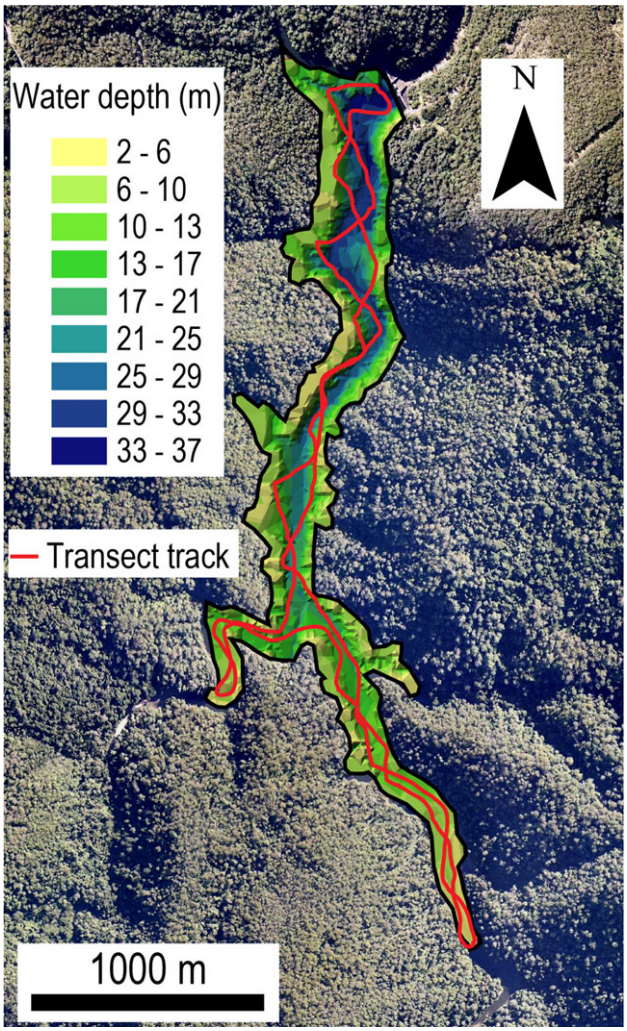

Figure 9. The bathymetry profile of Little Nerang Dam, Queensland, and the repeated sampling path followed by the *Wivenhoe* ASV (red).

implemented across multiple robots to improve spatial coverage with the possibility to exploit adaptive sample site selection sampling allowing exploration across water bodies. The following outlines the sampling approaches adopted in this paper for the two systems.

5.1. Single ASV Repeat Transects

The OMD-based methane measurement approach described in Section 4.1 exploits the *Wivnehoe* ASV's ability to repeatedly follow a transect in order to obtain continuous spatial coverage and temporal measurements across an entire water body.

For the results presented in Section 6, a predefined transect across a water reservoir (Little Nerang Dam, Queensland, Australia), shown in Figure 9 was specified for the ASV. Because of the potential errors in localization resulting from multipathing of GPS signals from the steep-sided catchment (particularly in the Eastern and Western distal arms) and significant disturbances from strong winds, the ASV required real-time reactive obstacle detection and avoidance for safe navigation. Details of the obstacle avoidance and general tracking performance are presented in previous work (Dunbabin & Grinham, 2010).

This ability to follow repeat transects allows capture of the spatial and temporal characteristics of methane ebullition across the entire waterway.

5.2. Multi-robot Sample Site Selection

The GSS-based multi-robot system utilizes a set of smaller *Inference* ASVs to collect static measurements over space and time. While the system can implement repeat transects, its slower measurement rate (due to the required stationary sampling incubation time) and slower travel speeds mean that continuous measurements along a path is not feasible at the scale of the process being observed (see Section 1). As such, it is considered more amenable to use multiple sensing assets and adaptive path planning approaches, particularly for previously unexplored environments to improve spatial and temporal coverage.

In this study, to demonstrate the sampling system concepts, a simplified random walk-based algorithm is proposed for selecting locations for n ASVs to sample the environment in an attempt to identify regions with high methane gas flux. There are two key assumptions: (1) the boundary of the water body is known from sources such as GIS, and (2) the ASVs can communicate between each other and can share their list of previous and next sample locations. In this study, we did not use bathymetry, but it could be used in the future to help guide the algorithm.

The selection of new sample locations is based on an online random walk and potential fields. Iterating through each robot, the basis of the algorithm is as follows:

1. All previously sampled sites for all robots are represented as two-dimensional Gaussian potentials centered at those points with fixed amplitude and standard deviation.
2. A random position at radius r from the current position is selected. If this position is not on land, and the value from the closest Gaussian potential is less than a threshold, this becomes the next sample point for that robot. If this condition is not met, the process is iterated until a location can be found. If no location can be found after a set number of iterations, the search radius is increased by Δr and the process repeated until a site is found or some termination criteria are met.
3. To increase local intensification of sampling in methane "hot-spots", if the measured flux rate at the robot's current location exceeded some threshold, the search radius

for the next sample step is set to βr, where $(0 < \beta \leq 1)$ and the potential threshold trigger relaxed.

The values of r, β, and number of samples in this study were arbitrarily chosen based on experience at these reservoirs to demonstrate the approach within a reasonable time frame while attempting to span the entire reservoir. Selections of more optimal values of these parameters are possible avenues for future research.

Once the new set of sample locations (waypoints) for each robot is calculated, each robot then drives in a straight line toward the goal. If the water depth falls below a threshold (i.e., too shallow) or an obstacle is detected, the vehicle starts to move either clockwise or counterclockwise around the contour until a new straight line to the goal can be achieved. This entire process is repeated for all robots until a desired number of samples are collected or some other termination condition is met.

6. RESULTS

A series of experimental campaigns with both the *Wivenhoe* and *Inference* ASV systems have been conducted on Little Nerang Dam (LND) in South East Queensland (S28°08.628′ E153° 17.085′) to evaluate the complementary greenhouse gas sampling methodologies above. This drinking water reservoir is a narrow waterway with a steep-sided catchment having a surface area of 0.5 km^2 and mean depth of 14 m. LND is an established study site and was selected because it consistently exhibits regions of significantly high methane ebullition and provides a range of challenging operational conditions for evaluating robotic systems. Experimental results from validation campaigns in 2009 (*Wivenhoe*) and 2015 (*Inference*) are presented below.

6.1. Single-ASV Bubble Detection

The *Wivenhoe* ASV fitted with the OMD was tasked with performing repeated transects that crisscross the entire reservoir from the Northern dam wall and then south through both distal arms and back to the dam wall. Figure 9 shows the transect that was repeated by the ASV (shown in red) and the prerecorded bathymetry profile of the reservoir.

In total, seven transects were conducted over 3 days in October 2009 to evaluate the spatiotemporal ebullition characteristics. Each transect was approximately 7.8 km in length and took on average 149 min to complete. During the missions, the OMD-based ebullition detection system of Section 4.1 was used to identify when bubbles were detected and to estimate the associated bubble size and volume of methane. Each detected methane bubble was georeferenced based on the ASV's GPS position. Figure 10 illustrates the rate of detected bubble volume from two of the transects (midday and morning mission). As can be seen, the spatial extent of the region where bubbles were detected varies significantly in addition to rate of the detected bubbles.

A summary of the results from all seven transects is given in Table III, showing the number of detected bubbles, the mean bubble volume, and an estimation of the ebullition zone. In this study, the ebullition zone (i.e., the estimated surface area that is emitting bubbles) is calculated by gridding the entire water storage into 20 m × 20 m cells and summing all cells in which a bubble was detected. As can be seen, there is significant variability in the number of detected bubbles and their volume, as well as the spatial extent between each transect (several hours). This spatial and temporal variation of methane ebullition, which we can visually observe on the water's surface on as little as 30-min timescales when in the field, illustrates the difficulty in accurately quantifying this process using fixed point sampling. It also highlights the need to perform repeated transects over long periods of time to understand the true spatiotemporal variability of methane release to the atmosphere. The location of all detected bubbles using this approach from all the transects along with the estimated methane flux rate to atmosphere is shown in Figure 13(a).

In addition to being able to localize the detected bubble, the system also allows the detected bubbles to be characterized in terms of other measured parameters from the ASV. For example, Figure 11 shows the cumulative distribution of detected bubbles against the depth of water at their detection location for all seven transects. The majority of detected bubbles occur in less than 5 m water depth. The results shown in Figure 11 is consistent with limited published results on methane ebullition using manual measurement technique (Joyce & Jewell, 2003). This information could potentially be used to generate utility functions for use in future adaptive sampling algorithms for both the OMD and GSS-based sampling approaches to improve the efficiency of monitoring and quantification programs.

The OMD-based method of methane ebullition detection and quantification provides a repeatable continuous measurement to provide unique spatial and temporal maps of methane hot spots. However, the size, weight, and operating power of the OMD (60 W) required the use of a larger platform, such as the *Wivenhoe* ASV. The *Wivenhoe* ASV has an effective energy capacity of 2,016 Wh stored in two onboard lead-acid batteries and 300 W of solar panels. However, because of the tight maneuvering required, particularly in the distal arms of LND, the average power consumption for propulsion, computing, and payload was estimated at 491 W. This limited the ASV to only two transects before charging or replacement of the batteries was deemed necessary in the experimental campaign (see Section 6.3.2 for further discussion).

6.2. Multi-ASV Gas Sampling

During January to May 2015, a series of experimental trials of the *Inference* ASVs were conducted on Little Nerang

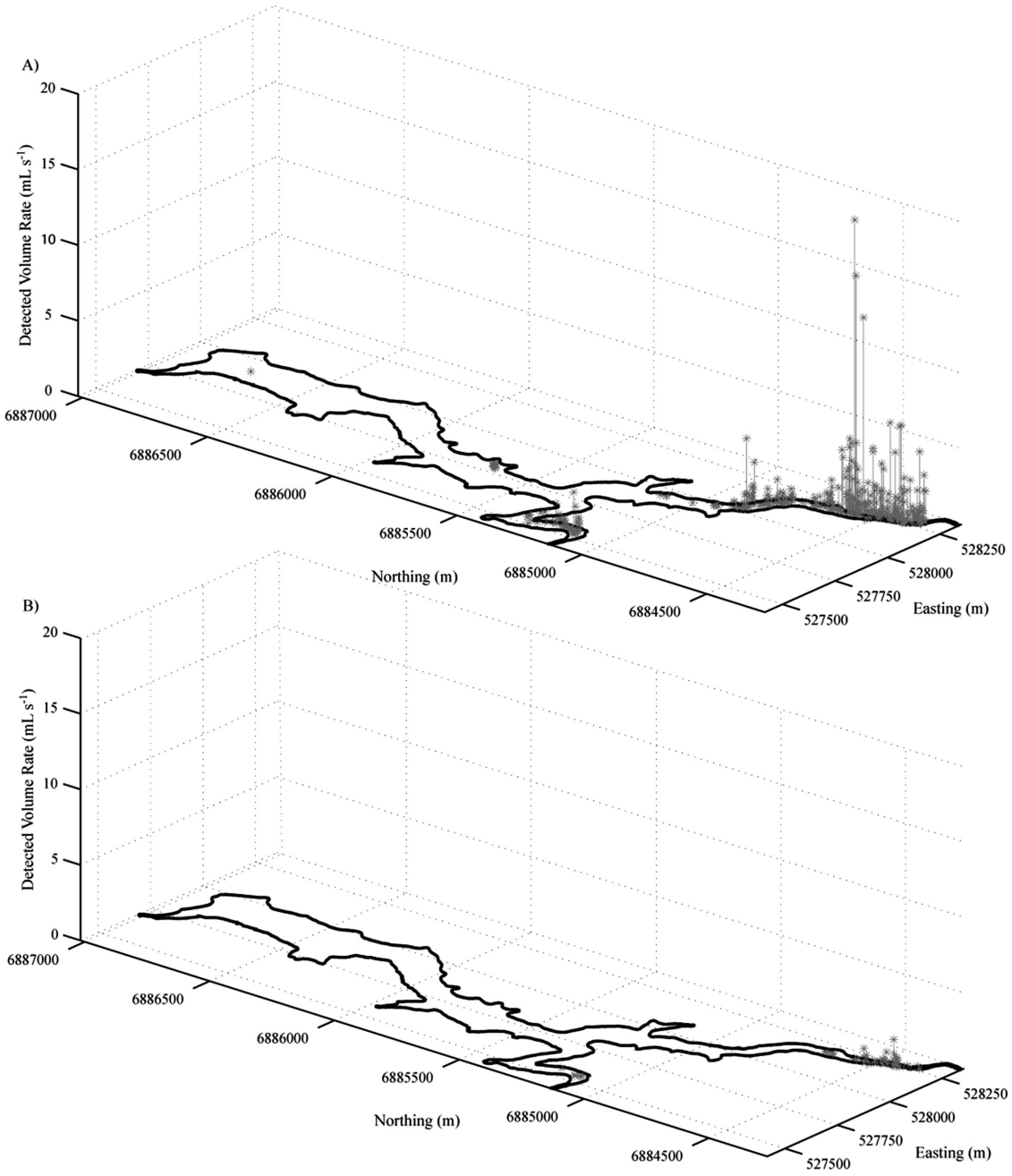

Figure 10. Illustration of the variability in the number of bubble and their spatial and the calculated methane volume rate using the proposed OMD method for a midday transect (Run 1), and a morning transect (Run 3). Shown is the outline of the water reservoir (black) and the calculated volume rate (vertical gray lines).

Dam, Gold Creek Reservoir (S27° 27.583′ E152°52.753′) and Hinze Dam (S28° 03.413′ E153° 16.921′) to evaluate different aspects of their sampling, navigation, and station keeping performance as well as power consumption.

Two of the four *Inference* ASVs were fitted with GSS units and used in the evaluation trials. During navigation trials, the ASVs implemented the controller as described in (Dunbabin & Grinham, 2010) and were commanded to

Table III. Summary of the number of detected methane bubbles, mean bubble volume, and estimated ebullition zone for each transect of the ASV using the OMD-based method described in Section 4. Values represent totals or average ± SE..

Transect	Day, Start Time AEST	Number of detected bubbles	Bubble volume (mL)*	Ebullition zone area (m^2)
Run 1	Day 1, 12:36	421	2.23 ± 0.32	34,000
Run 2	Day 1, 16:08	104	0.74 ± 0.14	15,200
Run 3	Day 2, 07:44	70	0.34 ± 0.05	9,200
Run 4	Day 2, 10:20	183	2.09 ± 0.44	23,200
Run 5	Day 2, 16:17	54	0.39 ± 0.48	8,800
Run 6	Day 3, 08:48	103	2.94 ± 0.48	8,800
Run 7	Day 3, 11:54	159	0.68 ± 0.08	13,600

*Equivalent 100% methane concentration.

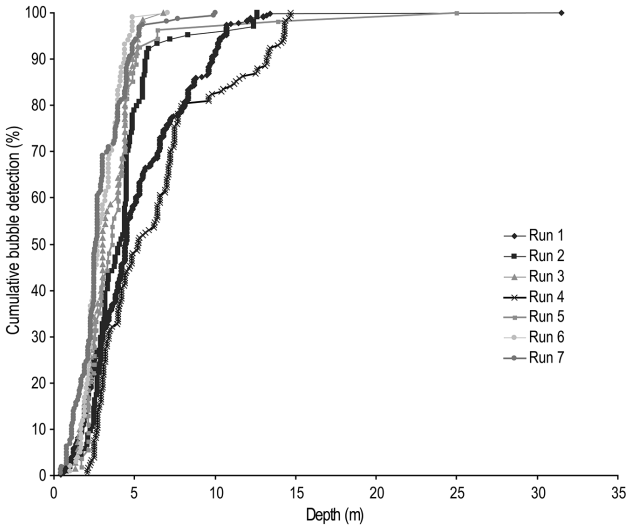

Figure 11. The cumulative distribution of detected methane bubbles against water depth using the *Wivenhoe* ASV and OMD-based measurement system for all transects (Modified from (Grinham et al., 2011)).

Figure 12. Two *Inference* ASVs fitted with GSSs during testing in South East Queensland. The retracted gas sampling unit is visible underneath the ASV on the right.

undertake a series of linear transects. The mean cross-track error was calculated to be 2.8 m using the ASV's onboard GPS position as ground truth with an average speed of 0.7 ms^{-1}. The average power required to achieve this tracking and speed performance was estimated to be 43 W.

The ASVs are required to remain effectively stationary during the incubation period of the gas sampling protocol. This requires an ability to "station-keep" at a GPS location. However, the ASVs only have two fixed thrusters for differential steering with no means for lateral control. Additionally, during station-keeping the motors should also not generate too much local turbulence as that may affect the gas measurement, particularly in shallow water. Therefore, in this study a "weak" station-keeping protocol was implemented whereby when the ASV is within 10 m of the desired sample location, it turns to align its bow or stern (taking smallest alignment angle) directly toward the goal. It then moves forward or backward (depending on the closest alignment) with the maximum allowable thrust decreased linearly with distance to the goal. No integral action was currently added to remove offsets due to wind or other disturbances. This simple strategy proved effective in practice with a mean position error of 3.1 m achieved based on the ASVs onboard GPS position (see Section 6.3.3 for further discussion). The average power consumption during station-keeping was estimated at 7.6 W for the conditions experienced at the water reservoirs considered here.

An experimental evaluation of the multi-ASV sampling protocol using the two *Inference* ASVs with gas sampling payloads (see Figure 12) was conducted on Little Nerang Dam. Using previously collected georeferenced outlines of the water's edge (boundary) the sample site selection algorithm described in Section 4 was implemented. Note only the boundary of the reservoir and not the bathymetry was used in this study. The sample selection algorithm was run with a total of 30 samples for each ASV, a step radius of 200 m, an intensification factor of 0.5, and a 2D Gaussian

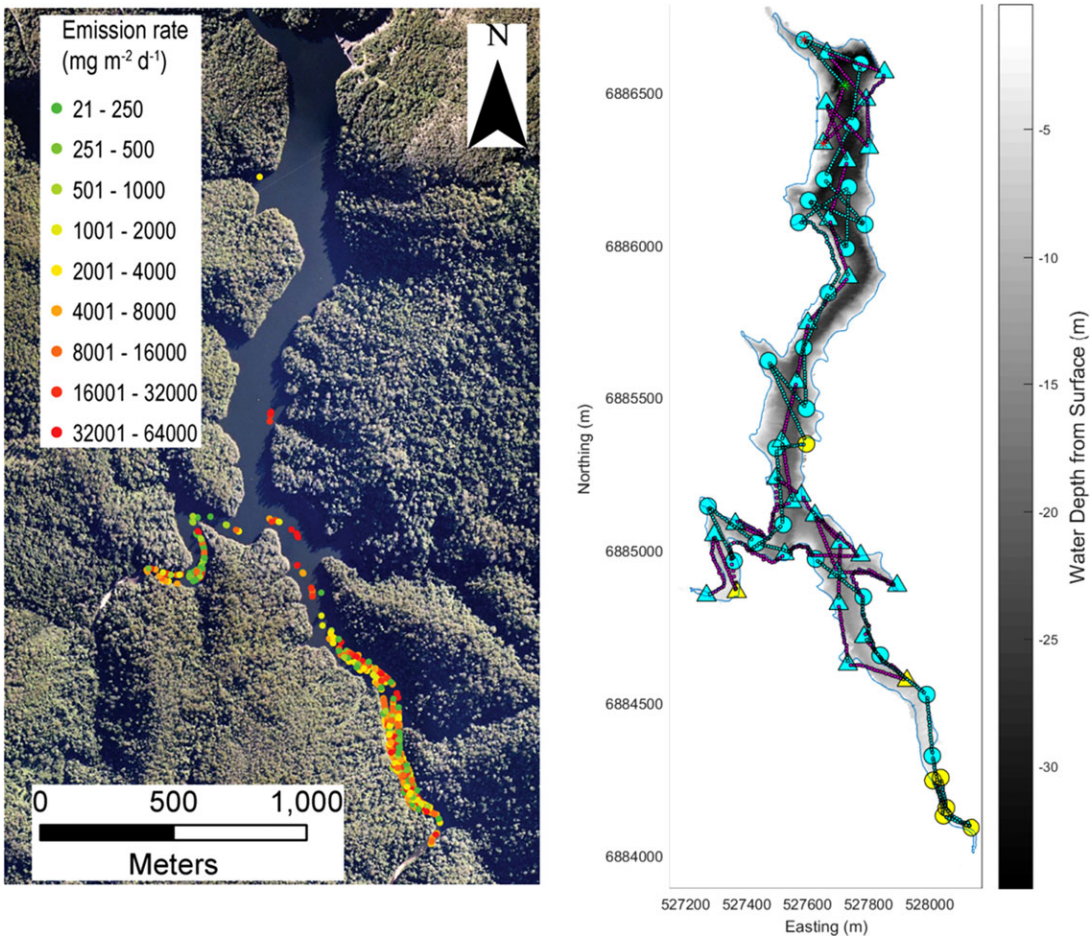

Figure 13. Sampling locations and ebullition detections from 15-min incubations using two ASVs on Little Nerang Dam, Queensland. Right: The trajectory and resulting sample locations indicated by the circles for ASV1 and triangles for ASV2. The start location for both ASVs was at the dam wall located at the northernmost end. The circles and triangles highlighted in yellow indicate the online chamber measurements that exceeded 1,000 mg m^{-2} d^{-1}. Left: An aerial image of Little Nerang Dam with all the OMD-based detected bubbles from all transects and estimated methane flux rate to atmosphere overlaid showing the regions dominated by methane ebullition.

potential standard deviation of 20 m (see Section 5.2). These values were chosen based on prior experience of the spatial extent of the ebullition zone as described above and to attempt to span the entire storage in a fixed time. The trigger value was set at 1,000 mg m^{-2} d^{-1} with 15 min incubations. The time to complete the experiment was approximately 10.5 hr. Figure 13(b) shows the results of implementing the sample strategy for both ASVs. These results show the ASV's ability to implement the sample protocol to explore and navigate the water reservoir.

The online detections of methane exceeding the trigger threshold (markers in yellow) was 8 times. Although the spatial density of exceedances are less than that from the previous OMD-based campaign, their location is consistent with the results collected by the OMD-based system (Figure 13(a)). As ebullition is difficult to predict and model (see Section 1), a number of factors may have contributed to the lower observed ebullition rate, including a higher dam level between the campaigns (approximately 2 m) and lower wind activity to cause internal disturbances. Qualitatively, the visible activity was less than in prior campaigns, and as such, the likelihood of placing a sensor in an ebullition zone is reduced. However, this does reinforce the need to have multiple assets simultaneously sampling the environment to capture these spatially and temporally discrete events.

Although the random walk algorithm implemented in this experiment achieved reasonably good coverage of the reservoir, it did highlight some general deficiencies of the approach. First, there is no guarantee that complete coverage will be achieved given a fixed number of samples. For

example, as seen in Figure 13, only ASV1 travels into the Southern reaches of the Eastern distal arm, whereas both ASVs collected sampled in the Western distal arm. Furthermore, the spatial coverage is not balanced as seen toward the middle of the reservoir where both ASVs selected sample locations close to the Western bank. In terms of the modification of the step size between samples, from the 60 samples collected, 50 were at 200 m, 5 were at 100 m, 4 were at 250 m, and 1 at 300 m. This illustrates in this particular case that spatial density of samples was not significantly high to force larger separation of future samples. Also, even though eight methane threshold exceedances were observed, only five resulted in the reduced 100 m step sizes as part of the intensification component of the algorithm. This was later determined to be the result of the algorithm not being able to randomly select a sample point at that radius within the set number of iterations allowed due to the step radius (r) being greater than the width of the narrow Southern arm. As such, the radius was increased by Δr, in this case 50 m, and the process repeated until a valid sample location was found. Whereas the random walk approach presented here demonstrated an ability to sample across a reservoir, future work will focus on more robust and optimal selection of the sample selection parameters.

6.3. Discussion and Lessons Learned

6.3.1. Ebullition Identification and Quantification

The results above illustrate that both proposed ASV-based greenhouse gas sampling methods are able to identify methane hot spots and quantify methane release due to ebullition. As ebullition is essentially a point-source emitter, there can be extreme variability even at short spatial and temporal scales (Grinham et al., 2011). Therefore, although ebullition can often be seen in expected regions (e.g., left image of Figure 13), a sample within that region does not always guarantee the capture of gas bubbles sufficient to achieve high rates. However, the systems proposed here provide complementary sensing capabilities, which could be combined to more efficiently measure the spatiotemporal variability of both ebullition and diffusion over long periods of time. This persistent monitoring is necessary on these reservoirs in order to obtain estimates of total annual methane emissions.

Whilst the experiments using the *Inference* ASVs demonstrated the system for real-time sampling of greenhouse gases across water bodies, the online component of gas sampling system was not optimized for detecting lower (and more common) flux rates of less than 1,000 mg m^{-2} d^{-1}. Future work will look at adaptive chamber head-space control as well as higher precision sensors to improve the utility of the system for accurate quantification of the combined diffusive and ebullitive flux of greenhouse gases.

6.3.2. Power Harvesting for Persistent Sampling

As described above, the detection and quantification of methane ebullition requires long-term spatial and temporal sampling. This in turn requires persistence. Even though the *Wivenhoe* ASV is able to provide continuous and large area coverage for methane detection, its power requirements limits the endurance, even with solar power, to less than 24 hr. However, the daily averaged power consumption for the *Inference* ASV for the experimental scenario described in Figure 13 was estimated to be 15.9 W. This overall lower power consumption gives the ASV an endurance of approximately 16 hr without any recharging and allows the possibility of effectively having permanent operation on the water storage using solar power harvesting.

In May 2015, a set of light loggers (Odyssey, Christchurch, New Zealand) were placed around LND to measure incoming solar radiation. Figure 14 shows an example of the measured solar radiation across the daylight hours at three sites: (1) the dam wall (northernmost point), (2) against the Eastern bank midway down the storage, and (3) at the Southern end of the Eastern distal arm. As can be seen, due to shadowing from the steep-sided catchment walls and tree cover, the amount of solar power available varies with time of day and location.

An estimation of the energy harvesting potential for each of the daily solar radiation cases shown in Figure 14. It was assumed that the ASV would remain at each of the three sites and was based on the current *Inference* ASV design with the maximum 80 W of panels and 15% solar conversion efficiency. For each of the three sites, the estimated daily averaged power harvest is 19.3, 10.1, and 15.9 W, respectively. As the current daily average power requirements for 15 min incubation sampling is 15.9 W, and given that only 34% of the ASVs top deck is currently covered in solar panels, there is potential to achieve long-term sampling endurance with the addition of more solar panels. Current research is focused on developing multi-robot sampling strategies that consider power harvesting potential to maintain persistent observation in such light-varying conditions.

6.3.3. Lessons Learned

Throughout the experimental campaigns described above and greater experience with these two ASV systems, a number of unexpected observations were made and conditions encountered that have improved our designs and operations over time.

For example, during a weeklong power harvesting and sampling experiment in May 2015, one of the *Inference* ASVs suffered complete electronics failure due to a nearby lightning strike during a storm event. Similar failures had occurred on static sensor nodes in the past, with the fix now being the addition of a lightning arrestor to the communications antenna. Even though the ASV was anchored at the time, this also highlighted the need for safety systems

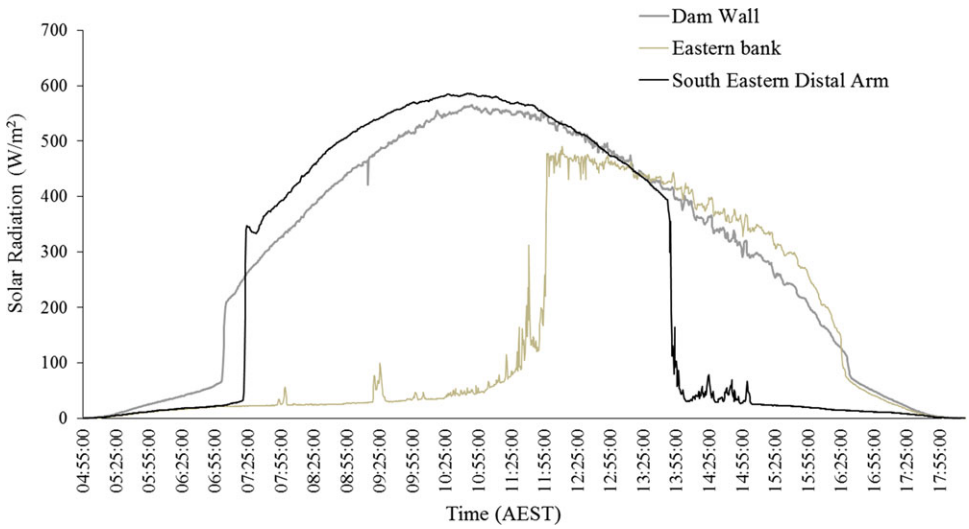

Figure 14. Measured solar radiation across a day at three locations on Little Nerang Dam showing the effect of shadows due to the steep-sided catchment.

that include an ability to automatically drop a restraining anchor so that the vehicle does not drift downstream in the event of motor or electronics failure, or if the ASV breaches a geo-fence.

In terms of large-scale and persistent sampling, it is important to be able to validate online measurements with physical samples, which can be processed in a laboratory using established methods. Even though the *Inference* ASV has a vial system for capturing physical gas samples, its carrying capacity was limited to six vials. When conducting larger campaigns such as considered here, a larger number of vials are needed and requires a modified design. For the OMD-based system, the sensor itself was observed to cause problems with its measurement at night. During nighttime trials, the relatively intense sensor light of the OMD attracted a large number of insects (e.g., moths), which corrupted the measurements as they flew into the sensor field-of-view. Therefore, a screen was needed and constructed with gaps small enough to stop insects but not disrupt gas flow through the sensor.

A particular issue on LND was the inconsistency of GPS coverage and multipathing. This is due to the relatively lower number of satellites over the Southern Hemisphere and lack of augmentation systems, as well as the physical terrain characteristics (steep-sided catchment). As the two ASV systems used GPS as a primary navigation sensor, any significant drift in position could potentially cause the ASVs to drift onto the sides of the reservoir or into regions with difficult to see obstacles (e.g., water lilies at night). This may also become a problem during station-keeping when close to these regions. The *Wivenhoe* ASV trials was observed to suffered more GPS signal degradation than the *Inference* ASV trials; however, its laser-based obstacle detection proved very effective in maintaining safe distances from the bank. The *Inference* ASVs have less sophisticated obstacle detection systems, and therefore, as general practice the georeferenced boundary is made more conservative particularly in the Southern distal arms to keep away from the sides in anticipation of degraded GPS.

7. CONCLUSIONS

This paper described and evaluates two robotic sampling systems for conducting large-scale monitoring of a greenhouse gas (methane) on complex inland waterways. The multi-robot system, named *Inference*, consists of multiple networked ASVs carrying a custom-developed greenhouse gas sampling payload to provide discrete methane measurements across a water reservoir. This multi-robot system was compared to a complementary approach based on a single larger ASV, named *Wivenhoe*, fitted with an OMD and implementing an algorithm to detect and quantify methane bubbles that are released to the atmosphere as it travels over them. Field experiment results are shown that demonstrate each ASV's ability to navigate complex waterways and detect, localize, and quantify regions of high methane emissions to atmosphere. The results show that methane ebullition is strongly spatially and temporally varying, requiring persistent and distributed measurements. Future research is focused on developing more sophisticated multi-robot adaptive sampling algorithms to achieve persistent monitoring and mapping of spatiotemporal processes while considering energy, speed, and sampling constraints of the vehicles. In addition, new sensors and algorithms for headspace control of the GSS are being developed to improve

its lower detection limit for sampling regions with low gas flux rates.

ACKNOWLEDGMENTS

The authors would like to thank Katrin Sturm from the University of Queensland and Deborah Gale from Seqwater for their assistance with the field testing of the ASV prototypes and initial gas sampling unit evaluation and laboratory processing of gas samples. Also thanks to Riki Lamont for his assistance in the payload integration and commissioning of the Inference ASVs. Experiments using the OMD-based system were conducted while Matthew Dunbabin was working with the CSIRO.

REFERENCES

Bastviken, D., Tranvik, L., Downing, J., Crill, P., & Enrich-Prast, A. (2011). Freshwater methane emissions offset the continental carbon sink. Science, 331(6013), 50.

Beychok, M. R. (2005). Fundamentals of stack gas dispersion (4th ed.). Newport Beach, CA: Milton R. Beychok.

Borrel, G., Jezequel, D., Biderre-Petit, C., Morel-Desrosiers, N., Morel, J., Peyret, P., Fonty, G., & Lehours, A. (2011). Production and consumption of methane in freshwater lake ecosystems. Research in Microbiology, 162(9), 832–847.

Boudreau, B., Algar, C., Johnson, B., Croudace, I., Reed, A., Furukawa, Y., Dorgan, K., Jumars, P., Grader, A., & Gardiner, B. (2005). Bubble growth and rise in soft sediments. Geology, 33, 517–520.

Corke, P., Sikka, P., Roberts, J., & Duff, E. (2004). DDX: A distributed software architecture for robotic systems. In Proc. Australian Conf. Robotics and Automation, Canberra.

Crawford, J., Stanley, E., Spawn, S., Finlay, J., Loken, L., & Striegl, R. (2014). Ebullitive methane emissions from oxygenated wetland streams. Global Change Biology, 20, 3408–3422.

Dunbabin, M. (2015). Autonomous greenhouse gas sampling using multiple robotic boats. In Proc. Tenth International Conference on Field and Service Robotics (FSR), pp. 1–14. Toronto.

Dunbabin, M., & Grinham, A. (2010). Experimental evaluation of an autonomous surface vehicle for water quality and greenhouse gas monitoring. In Proc. International Conference on Robotics and Automation, pp. 5268–5274. Anchorage, Alaska.

Dunbabin, M., Grinham, A., & Udy, J. (2009). An autonomous surface vehicle for water quality monitoring. In Proc. Australasian Conference on Robotics and Automation. Sydney, Australia.

Dunbabin, M., & Marques, L. (2012). Robots for environmental monitoring: Significant advancements and applications. Robotics Automation Magazine, IEEE, 19(1), 24–39.

Duranti, P. (2015). Engineering geology for society and territory: Vol. 3. River basins, reservoir sedimentation and water resources, chapter 129: CatOne, Multitask unmanned surface vessel for hydro-geological and environment surveys (pp. 647-652). Cham, Switzerland: Springer International.

Ferreira, H., Almeida, C., Martins, A., Almeida, J., Dias, N., Dias, A., & Silva, E. (2009). Autonomous bathymetry for risk assessment with ROAZ robotic surface vehicle. OCEANS 2009 - EUROPE, pp. 1–6. doi: 10.1109/OCEANSE.2009.5278235.

Garneau, M.-E., Posch, T., Hitz, G., Pomerleau, F., Pradalier, C., Siegwart, R., & Pernthaler, J. (2013). Short-term displacement of Planktothrix rubescens (cyanobacteria) in a pre-alpine lake observed using an autonomous sampling platform. Limnology and Oceanography, 58(5), 1892–1906.

Girdhar, Y., Xu, A., Dey, B. B., Meghjani, M., Shkurti, F., Rekleitis, I., & Dudek, G. (2011). MARE: Marine autonomous robotic explorer. In Intelligent Robots and Systems (IROS), 2011 IEEE/RSJ International Conference on, pp. 5048–5053. San Francisco, California, USA.

Grinham, A., Dunbabin, M., Gale, D., & Udy, J. (2011). Quantification of ebullitive and diffusive methane release to atmosphere from a water storage. Atmospheric Environment, 45(39), 7166–7173.

Hitz, G., Pomerleau, F., Garneau, M.-E., Pradalier, C., Posch, T., Pernthaler, J., & Siegwart, R. (2012). Autonomous inland water monitoring: Design and application of a surface vessel. Robotics Automation Magazine, IEEE, 19(1), 62–72.

Hombal, V., Sanderson, A., & Blidberg, D. (2010). Multiscale adaptive sampling in environmental robotics. In Multisensor Fusion and Integration for Intelligent Systems (MFI), 2010 IEEE Conference on, pp. 80–87. Salt Lake City, UT, USA.

Joyce, J.& Jewell, P. (2003). Physical controls on methane ebullition from reservoirs and lakes. Environmental and Engineering Geoscience, 9, 167–178.

Leedekerken, J., Fallon, M., & Leonard, J. (2014). Mapping complex marine environments with autonomous surface craft. In Experimental Robotics, volume 79 of Springer Tracts in Advanced Robotics, pp. 525–539. Berlin: Springer.

Louis, V. S., Kelly, C., Duchemin, E., Rudd, J., & Rosenberg, D. (2000). Reservoir surfaces as sources of greenhouse gases to the atmosphere: A global estimate. BioScience, 50, 766–775.

Maeck, A., Hofmann, H., & Lorke, A. (2014). Pumping methane out of aquatic sediments-ebullition forcing mechanisms in an impounded river. Biogeosciences, 11, 2925–2938.

Manley, J., & Willcox, S. (2010). The wave glider: A persistent platform for ocean science. In OCEANS 2010 IEEE - Sydney, pp. 1–5. Sydney, Australia.

McGinnis, D., Greinert, J., Artemov, Y., Beaubien, S., & Wuest, A. (2006). Fate of rising methane bubbles in stratified waters: How much methane reaches the atmosphere? Journal of Geophysical Research, 111, 1–15.

Rynne, P., & Ellenrider von, K. (2008). A wind and solar-powered autonomous surface vehicle for sea surface measurements. In Proc. IEEE OCEANS 2008, pp. 1–6. Kobe, Japan.

Savvaris, A., Oh, H. N. H., & Tsourdos, A. (2014). Collision avoidance algorithms for the c-enduro USV. In The 19th World Congress-The International Federation of Automatic Control, pp. 12174–12181. Cape Town, South Africa.

Scherer, S., Rehder, J., Achar, S., Cover, H., Chambers, A., Nuske, S., & Singh, S. (2012). River mapping from a flying robot: State estimation, river detection, and obstacle mapping. Autonomous Robots, 33(1-2), 189–214.

Tokekar, P., Branson, E., Hook, J. V., & Isler, V. (2013). Tracking aquatic invaders: Autonomous robots for monitoring invasive fish. IEEE Robotics Automation Magazine, 20(3), 33–41.

Valada, A., Velagapudi, P., Kannan, B., Tomaszewski, C., Kantor, G. A., & Scerri, P. (2012). Development of a low cost multi-robot autonomous marine surface platform. In The 8th International Conference on Field and Service Robotics (FSR 2012).

Wang, J., Gu, W., & Zhu, J. (2008). Design of an autonomous surface vehicle used for marine environmental monitoring. In Proc. International Conference on Advanced Computer Control (ICACC09), pp. 405–409.

Yoo, S.-H., Stuntz, A., Zhang, Y., Rothschild, R., Hollinger, G., & Smith, R. (2015). Experimental analysis of receding horizon planning algorithms for marine monitoring. In Proc. Tenth International Conference on Field and Service Robotics (FSR), pp. 1–14. Toronto.

Zhang, B., & Sukhatme, G. (2007). Adaptive sampling for estimating a scalar field using robotic boat and a sensor network. In Proc. International Conference on Robotics and Automation, pp. 3673–3680. Roma, Italy.